DOI: 10.1021/cg100927k

CRYSTAL GROWTH & DESIGN Article
XXXX, Vol. XXX
000–000

Encapsulated Diverse Water Aggregates in Two Ag(I)/4,4′-Bipyridine/Dicarboxylate Hosts: 1D Water Tape and Chain

Di Sun, Hao-Ran Xu, Cheng-Feng Yang, Zhan-Hua Wei, Na Zhang, Rong-Bin Huang,* and Lan-Sun Zheng

State Key Laboratory of Physical Chemistry of Solid Surface, Department of Chemistry, College of Chemistry and Chemical Engineering, Xiamen University, Xiamen 361005, China

Received July 14, 2010; Revised Manuscript Received August 24, 2010

ABSTRACT: Two mixed-ligand Ag(I) coordination polymers (CPs), namely, $[Ag_2(bipy)_2(ox)\cdot 7H_2O]_n$ (**1**) and $[Ag_2(bipy)_2(adip)\cdot 6H_2O]_n$ (**2**) (bipy = 4,4′-bipyridine, H_2ox = oxalic acid, H_2adip = adipic acid) have been synthesized and structurally characterized. Complex **1** exhibits a three-dimensional (3D) framework constructed from ox pillared Ag−bipy sheets. Complex **2** shows a stairlike two-dimensional (2D) structure composed of adip linked Ag−bipy double chains. Of particular interest, a 1D C4 water chain and a novel 1D T7(2) water tape constructed from edge-sharing heptamer water clusters coexist in complex **1**, while a 1D C6 water chain exists in complex **2**. Comparing the experimental results, it is comprehensible that the dicarboyxlates play crucial roles in the formation of the diverse structures and water aggregates. Additionally, results about thermogravimetric curves and photoluminescence spectra were discussed.

Introduction

There is hardly a compound which has captured more interest than water, because of its fundamental importance in many biological and chemical processes. Theoretical and experimental studies on the structural and dynamic properties of, for example, discrete water clusters, chains, and sheets, in vapor, water, and ice have been carried out to gain further insight into the structure of bulk water, which is poorly understood.[1] Assembly of discrete water aggregates and understanding how the water aggregates interact with the crystal host are still challenging scientific endeavors.[2] This consciousness has led to the exploration of several interesting water clusters $(H_2O)_n$,[2] as well as one-dimensional (1D) chains,[3] 1D tapes,[4] two-dimensional (2D) layers,[5] and three-dimensional (3D) water structures.[6] Among the discrete small water clusters, even-numbered water clusters such as tetramers,[7] hexamers,[8] octamers,[9] decamers,[10] dodecamers,[11] tetradecamers,[12] hexadecamers,[2a,13] octadecamers,[2n,p] and icosadecamers[2o] are common within the lattice of a crystal host. However, surprisingly little is known of the discrete odd-number water clusters, even though trimers[14] and pentamers[15] are familiar in crystal hydrates. Especially, the odd−number heptamer cyclic water seems to be a missing member and is rarely reported in experiments.[16] Although Buck et al. have proposed to detect only the cagelike heptamer[17] based on the infrared OH stretching vibrations in molecular beam depletion spectroscopy, and theoretical calculations were also performed on twelve possible water heptamer structures to explore the conformations as well as the spectroscopic properties of these water clusters,[18] the solid-state structure of the cyclic heptamer is still elusive.

However, a simple discrete water cluster is still not adequate for researchers to comprehend all branches of natural sciences. The 1D water extended structure plays very important roles in several biological processes.[19] The 1D water aggregates, chain and tape, can be constructed by an infinite connection of water molecules[3] or by linking of the same or different types of cyclic small water clusters.[20] The 1D tape lies between a discrete cluster (0D) and a 2D sheet and can be either vertex- or edge-sharing, which not only is a simplified model in a 2D sheet but also has a close approximation to ice in the small water clusters.[21] In fact, hitherto, the modulation of water aggregates is still a long-standing challenge,[5b,22] despite hydrogen-bonding interactions, and their fluctuations are well-known to determine the arrangement of water.

In our previous work on the Ag(I)/bipy/aryl-dicarboxylate system,[23] we only obtained some mixed H_2O−dicarboxylate anionic sheets instead of pure water aggregates. Herein, we replaced aryl−dicarboxylates by aliphatic−dicarboxylates in the above system and obtained two CPs, namely, $[Ag_2(bipy)_2(ox)\cdot 7H_2O]_n$ (**1**) and $[Ag_2(bipy)_2(adip)\cdot 6H_2O]_n$ (**2**) (bipy = 4,4′-bipyridine, H_2ox = oxalic acid, H_2adip = adipic acid) (Scheme 1), which incorporate two different water aggregates (1D T7(2) water tape + 1D C4 water chain for **1** and 1D C6 water chain for **2**).

Experimental Section

Materials and General Methods. All chemicals and solvents used in the syntheses were of analytical grade and used without further purification. IR spectra were measured on a Nicolet 330 FTIR spectrometer in the range 4000−400 cm^{-1}. Elemental analyses were carried out on a CE instruments EA 1110 elemental analyzer. Photoluminescence spectra were measured on a Hitachi F-4500 fluorescence spectrophotometer (slit width, 5 nm; sensitivity, high). TG curves were measured from 25 to 800 °C on a SDT Q600 instrument at the heating rate 5 °C/min under N_2 atmosphere (100 mL/min). X-ray powder diffractions were measured on a Panalytical X-Pert pro diffractometer with Cu Kα radiation.

Preparation of Complexes 1 and 2. $[Ag_2(bipy)_2(ox)\cdot 7H_2O]_n$ (1). A mixture of $AgNO_3$ (167 mg, 1 mmol), bipy·$2H_2O$ (194 mg, 1 mmol), and H_2ox (90 mg, 1 mmol) was treated in CH_3OH−H_2O mixed solvent (10 mL, v/v: 1/1) under ultrasonic irradiation at ambient temperature. Then aqueous NH_3 solution (25%) was dropped into the mixture to give a clear solution. The resultant solution was allowed to evaporate slowly in darkness at ambient temperature for

*Corresponding author. E-mail: rbhuang@xmu.edu.cn. Fax: 86-592-2183074.

Scheme 1. 1D Water Tape/Chain Dependent on the Different Dicarboxylates

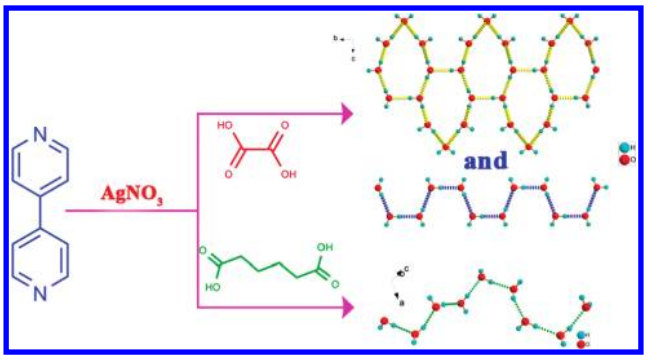

several days to give colorless crystals of **1** (yield: 83%, based on $AgNO_3$). They were washed with a small volume of cold CH_3OH and diethyl ether. Anal. Calcd for $Ag_2C_{22}H_{30}N_4O_{11}$: C, 35.60; H, 4.07; N, 7.55. Found: C, 35.52; H, 4.11; N, 7.59. Selected IR peaks (cm^{-1}): 3418 (s), 3042 (w), 2925 (w), 2852 (w), 1599 (s), 1410 (m), 1385 (s), 1312 (s), 1217 (m), 1070 (w), 990 (w), 803 (m), 617 (w), 506 (w).

$[Ag_2(bipy)_2(adip)\cdot 6H_2O]_n$ (2). Synthesis of **2** was similar to that of **1**, but using H_2adip (146 mg, 1 mmol) instead of H_2ox. Colorless crystals of **2** were obtained in 75% yield based on $AgNO_3$. Elemental analysis: Anal. Calcd for $AgC_{13}H_{18}N_2O_5$: C, 40.02; H, 4.65; N, 7.18. Found: C, 40.11; H, 4.71; N, 7.23. Selected IR peaks (cm^{-1}): 3430 (s), 3090 (w), 3038 (w), 1602 (s), 1532 (w), 1489 (w), 1385 (s), 1330 (m), 1217 (w), 1070 (w), 819 (m), 724 (w), 641 (w).

X-ray Crystallography. Single crystals of complexes **1** and **2** with appropriate dimensions were chosen under an optical microscope and quickly coated with high vacuum grease (Dow Corning Corporation) before being mounted on a glass fiber for data collection. Data were collected on a Rigaku R-AXIS RAPID Image Plate single-crystal diffractometer (Mo Kα radiation, λ = 0.71073 Å) equipped with an Oxford Cryostream low-temperature apparatus operating at 50 kV and 90 mA in ω scan mode for **1** and **2**. A total of 44 × 5.00° oscillation images was collected, each being exposed for 5.0 min. Absorption correction was applied by correction of symmetry-equivalent reflections using the ABSCOR program.[24] In all cases, the highest possible space group was chosen. All structures were solved by direct methods using SHELXS-97[25] and refined on F^2 by full-matrix least-squares procedures with SHELXL-97.[26] Atoms were located from iterative examination of difference F-maps following least-squares refinements of the earlier models. Hydrogen atoms were placed in calculated positions and included as riding atoms with isotropic displacement parameters 1.2−1.5 times U_{eq} of the attached C atoms. The hydrogen atoms attached to oxygen were refined with O−H = 0.85 Å, and U_{iso}(H) = 1.2U_{eq}(O). The hydrogen atoms of O1W (H1WA and H1WB) and O4W (H4WB and H4WC) for **1** and O1W (H1WA and H1WB), O2W (H2WB and H2WC), and O3W (H3WB and H3WC) for **2** are disordered with equal occupancy over two orientations related by the two-fold axis and inversion center for **1** and **2**, respectively. The C13 of adip is disordered over two sites with occupancy of 0.28 and 0.72. All structures were examined using the Addsym subroutine of PLATON[27] to ensure that no additional symmetry could be applied to the models. Pertinent crystallographic data collection and refinement parameters are collated in Table 1. Selected bond lengths and angles for **1** and **2** are collated in Table 2. The hydrogen bond geometries for **1** and **2** are shown in Table 3. CCDC-783994 (**1**) and CCDC-783995 (**2**) contain the supplementary crystallographic data for this paper. These data can be obtained free of charge from The Cambridge Crystallographic Data Centre via http://www.ccdc.cam.ac.uk/datarequest/cif.

Results and Discussion

Synthesis and General Characterization. The synthesis of complexes **1** and **2** was carried out in darkness to avoid photodecomposition. As is well-known, the reactions of Ag(I) with dicarboxylates in aqueous solution often result in the formation of microcrystalline or amorphous insoluble silver salts, presumably due to the fast coordination of the

Table 1. Crystal Data for 1 and 2

complex	**1**	**2**
formula	$Ag_2C_{22}H_{30}N_4O_{11}$	$AgC_{13}H_{18}N_2O_5$
M_r	742.24	390.16
crystal system	orthorhombic	triclinic
space group	*Pnna*	$P\bar{1}$
a (Å)	17.271(3)	7.8756(6)
b (Å)	7.5384(15)	10.7284(9)
c (Å)	21.382(4)	11.2127(8)
α (deg)	90	116.097(2)
β (deg)	90	93.149(2)
γ (deg)	90	110.295(3)
V (Å^3)	2783.8(9)	773.39(10)
T (K)	173(2)	173(2)
Z, D_{calcd} (g/cm^3)	4, 1.771	2, 1.675
F(000)	1488	394
μ (mm^{-1})	1.470	1.325
reflns collected/unique	31979/3183	6094/2725
R_{int}	0.1316	0.0261
parameters	177	206
final R indices [$I > 2\sigma(I)$]	R_1 = 0.0643[a]	R_1 = 0.0269[a]
	wR_2 = 0.1562[b]	wR_2 = 0.0667[b]
R indices (all data)	R_1 = 0.0784[a]	R_1 = 0.0291[a]
	wR_2 = 0.1646[b]	wR_2 = 0.0680[b]
goodness-of-fit on F^2	1.077	1.067

[a] $R_1 = \sum||F_o| - |F_c||/\sum|F_o|$. [b] $wR_2 = [\sum w(F_o^2 - F_c^2)^2]/\sum w(F_o^2)^2]^{1/2}$.

Table 2. Selected Bond Lengths (Å) and Angles (deg) for 1 and 2

	Complex **1**		
Ag1—N2^i	2.168(5)	Ag1—O1	2.616(6)
Ag1—N1	2.171(5)	N2^i—Ag1—O1	91.5(2)
N2^i—Ag1—N1	162.4(2)	N1—Ag1—O1	106.0(2)
Complex **2**			
Ag1—N2^i	2.2298(17)	Ag1—O1	2.7627(19)
Ag1—N1	2.2318(19)	Ag1—O2	2.7431(19)
N2^i—Ag1—N1	161.05(8)	N2^i—Ag1—O1	95.20(6)
N2^i—Ag1—O2	88.66(7)	N1—Ag1—O1	95.07(6)
N1—Ag1—O2	109.96(7)	O2—Ag1—O1	47.37(6)

Symmetry code: (i) $-x, y-{}^1/_2, z+{}^1/_2$. Symmetry code: (i) $x, y+1, z+1$.

Table 3. Hydrogen Bond Geometries for 1 and 2

D—H···A	D—H	H···A	D···A	D—H···A
Complex **1**				
O1W−H1WA···O1W^{ii}	0.85	2.07	2.719(17)	133
O1W−H1WB···O1W^{iii}	0.85	1.96	2.81(2)	177
O1W−H1WC···O2W^{iii}	0.85	1.90	2.752(11)	178
O2W−H2WA···O3W^{iv}	0.85	2.01	2.849(9)	171
O4W−H4WB···O4W^{v}	0.85	1.86	2.710(13)	178
O4W−H4WC···O4W^{vi}	0.85	2.17	2.796(12)	131
O2W−H2WB···O1	0.85	1.96	2.771(10)	159
O3W−H3WA···O2	0.85	1.97	2.806(7)	167
O4W−H4WA···O2	0.85	1.94	2.789(9)	178
Complex **2**				
O1W−H1WA···O1W^{iii}	0.85	2.10	2.848(5)	147
O1W−H1WB···O2W	0.85	1.98	2.831(3)	176
O2W−H2WB···O3W	0.85	2.03	2.838(3)	158
O2W−H2WC···O1W	0.85	2.00	2.831(3)	165
O3W−H3WB···O3W^{v}	0.85	2.02	2.856(4)	170
O3W−H3WC···O2W	0.85	1.99	2.838(3)	173
O1W−H1WC···O1	0.85	2.09	2.936(3)	176
O2W−H2WA···O1^{iv}	0.85	2.05	2.886(3)	166
O3W−H3WA···O2^{iii}	0.85	1.98	2.796(3)	160

Symmetry codes: (ii) $x, -y+{}^1/_2, -z+{}^3/_2$; (iii) $-x+{}^1/_2, -y+1, z$; (iv) $x, y+1, z$; (v) $-x+{}^1/_2, -y, z$; (vi) $x, -y+{}^1/_2, -z+{}^1/_2$. Symmetry codes: (iii) $-x+1, -y+1, -z$; (iv) $-x, -y+1, -z$; (v) $-x, -y, -z-1$.

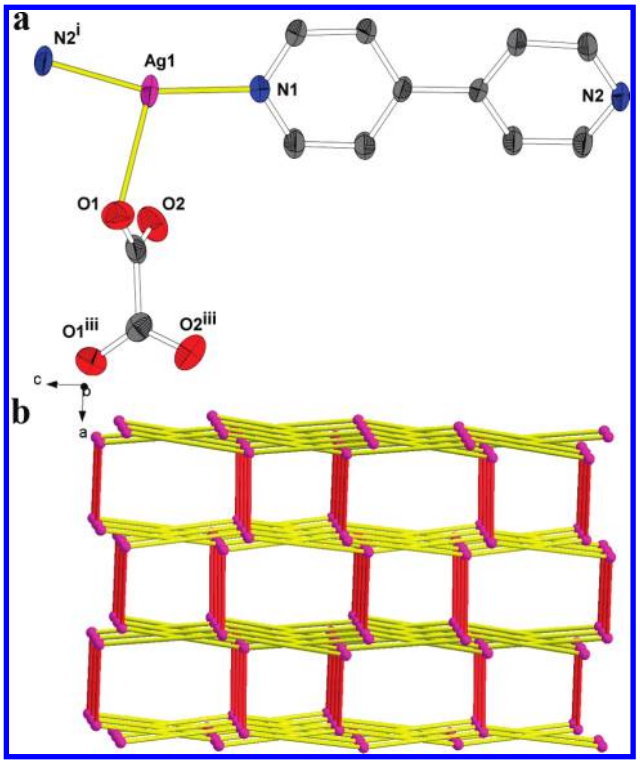

Figure 1. (a) Coordination environment of Ag(I) ion in **1** with the thermal ellipsoids at the 30% probability level. Hydrogen atoms and water molecules were omitted for clarity. (b) Presentation of the 3D network (red pillar, ox; yellow stick, bipy). (Symmetry codes: (i) $-x, y-{}^1/_2, z+{}^1/_2$; (iii) $-x+{}^1/_2, -y+1, z$.)

carboxylates to Ag(I) ions to form polymers.[28] Hence, properly lowering the reaction speed, such as using ammoniacal conditions, the layer-separation diffusion method, or even the gel permeation method, may favor formation of crystalline products.[29]

Powder X-ray diffraction (XRD) has been used to check the phase purity of the bulk samples in the solid state. For complexes **1** and **2**, the measured XRD patterns closely match the simulated patterns generated from the results of single-crystal diffraction data (Figure S1, Supporting Information), indicative of pure products. In the IR spectra (Figure S2, Supporting Information) of complexes **1** and **2**, the broad peaks at ca. 3400 cm^{-1} indicate the presence of water molecules. The IR spectra also show characteristic absorption bands mainly attributed to the asymmetric (ν_{as}: ca. 1600 cm^{-1}) and symmetric (ν_s: ca. 1385 cm^{-1}) stretching vibrations of the carboxylic groups. No band in the region 1690−1730 cm^{-1} indicates complete deprotonation of the carboxylic groups,[30] which is consistent with the result of the X-ray diffraction analysis.

Structure Descriptions. $[Ag_2(bipy)_2(ox)\cdot 7H_2O]_n$ (1). Single-crystal X-ray diffraction analysis reveals that complex **1** crystallizes in the space group *Pnna* and is an open 3D neutral network of rectangular channels with lattice water molecules. The overall network of **1** consists of Ag−bipy sheets and ox ligands as pillars. There are one Ag(I) ion, one bipy ligand, half an ox ligand, and three and a half water molecules in the asymmetric unit of **1**. The 2-fold axis passes through the midpoint of C11−C11^{iii} of ox and one water molecule (O3W). As depicted in Figure 1a, the Ag1 is located in a T-shaped geometry and coordinated by two symmetry independent N atoms from two bipy ligands (Ag1−O1 = 2.616(6), Ag1−N1 = 2.171(5), Ag1−N2^{i} = 2.168(5) Å). In addition to the strong coordination bonds, weak Ag···O interactions also exist (Ag1···O2 = 2.939(7) Å) which are a little longer but still fall in the secondary bonding range (the sum of van der Waals radii of Ag and O is 3.24 Å).[31] Both Ag−N and Ag−O bond lengths are well-matched to those observed in similar complexes.[32] The pyridyl rings of bipy ligand are noncoplanar, with a dihedral angle of 22.5(12)°. (Symmetry codes: (i) $-x, y-{}^1/_2, z+{}^1/_2$; (iii) $-x+{}^1/_2, -y+1, z$)

The Ag(I) ions are bridged by bipy ligands to form a 1D infinite polymeric chain structure. The interchain face-to-face $\pi\cdots\pi$ interactions ($Cg1\cdots Cg1^{vi}$ = 3.725(5) Å; $Cg1\cdots Cg2^{vii}$ = 3.748(5) Å; *Cg*1 and *Cg*2 are the centroids of aromatic ring N1/C1−C5 and N2/C6−C10; Figure S3 and Table S1) pack the 1D chains into the 2D sheets along the *bc* plane, which are further pillared by μ_2-η^1:η^0:η^1:η^0 ox to form the resulting neutral 3D framework (Figure 1b) with two different rectangular channels. The bigger one and the smaller one are assigned to channel A (12.8 × 7.7 $Å^2$) and B (8.7 × 7.7 $Å^2$), respectively. The dihedral angle between two symmetry-related carboxylic groups of ox is 99.7(8)°, which is surprisingly large and may be responsible for the staggered orientation of Ag−bipy chains between different sheets. Interestingly, a quick search of the Cambridge Structural Database (CSD)[33] for Ag−ox complexes reveals that ox ligand prefers to adopt a nearly planar geometry; however, only three examples, one reported by Kitagawa et al. ($[Ag_2(ppa)_2(ox)\cdot 9H_2O]_n$, ppa = *N*-(4-pyridinylmethyl)-4-pyridinecarboxamide)[34] and two reported by us ($[Ag_2$(2-aminopyrimidine)$_2(ox)\cdot 2H_2O]_n$[35a] and $[Ag_2$(2-aminopyrazine)$_2(ox)]_n$[35b]), are not the case, with dihedral angles of 63.4°, 58.4°, and 74.9°, respectively, between two carboxylic groups. The separation of Ag···Ag is 3.49 Å, which is slightly longer than twice the van der Waals radii of Ag(I), illustrating the lack of direct Ag···Ag interaction. (Symmetry codes: (vi) $x, -y+{}^1/_2, -z+{}^1/_2$; (vii) $x, -y+{}^3/_2, -z+{}^1/_2$.)

The most striking feature of **1** is the coexistence of the 1D water tape and the 1D water chain. As shown in Figure 2a, the hydrogen bonding association of water molecules leads to the formation of a cyclic heptamer with a pseudocrown conformation consisting of one independent O3W, two symmetry-related O2W, and four symmetry-related O1W. There is a crystallographic 2-fold axis along the *c* axis passing through this heptamer through O3W and the midpoint of O1W^{vii} and O1W^{viii}. As a result, the hydrogen atoms of O1W are disordered. In the heptamer, O3W acts as a double hydrogen bond acceptor and two O2W act as single hydrogen bond donor as well as acceptor. Of four O1W, three act in the same role to that of O2W, and the other one acts as a double hydrogen bond donor. The overall $(H_2O)_7$ cluster can be represented by $R_7^6(14)$ in the graph set notation,[36] and R7 by water cluster notation.[21a] As we know, hitherto, the only[16] crystallographically characterized heptamer water cluster exhibits a twisted-planar structure with a $R_5^5(14)$ hydrogen bond motif, which indicates the conformation of cyclic heptamer water in **1** is a new one. The hydrogen-bonded O···O separations in the heptamer span the range 2.710(13)−2.849(9) Å, with an average value of 2.773 (14) Å, which is comparable to 2.758 Å generated from the ab initio calculations.[37] As listed in Table 4, the O···O···O bond angles in heptamer are 127.0(3), 136.2(4), and 111.0(4)°, respectively, which are slightly different from the tetrahedral angle found in ice I_h and I_c,[11b] and the average torsion angle involving four adjacent water molecules is 43.2(7)°.

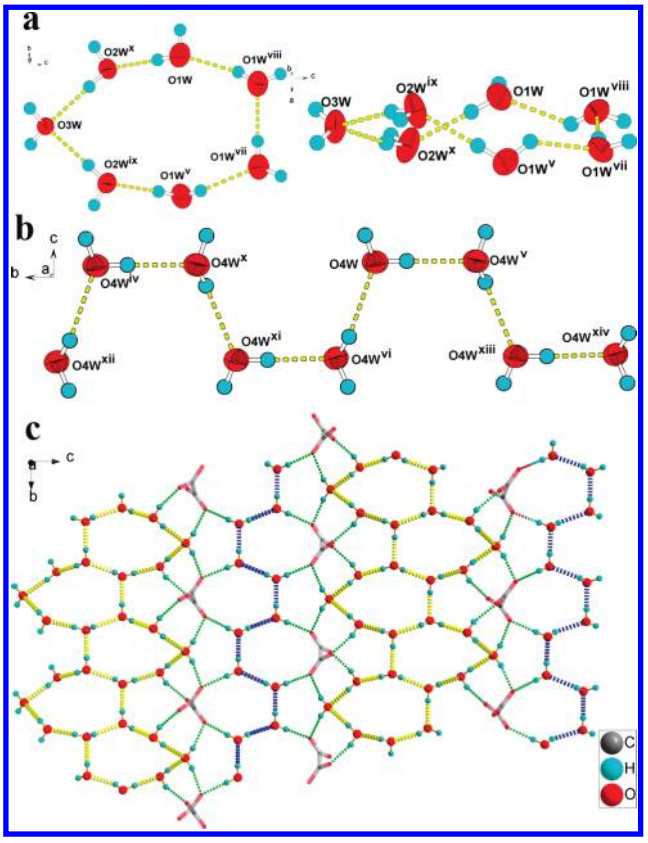

Figure 2. (a) ORTEP plot showing the single $(H_2O)_7$ cluster unit (left, top view; right, side view). (b) ORTEP plot showing the 1D water chain. (c) View of the 2D anionic sheet incorporating the T7(2) water tape (yellow dashed lines), the 1D C4 water chain (blue dashed lines), and ox ligands. (Symmetry codes: (iv) $x, y+1, z$; (v) $-x+{}^1/_2, -y, z$; (vi) $x, -y+{}^1/_2, -z+{}^1/_2$; (vii) $-x+{}^1/_2, y-{}^1/_2, -z+{}^3/_2$; (viii) $x, -y+{}^1/_2, -z+{}^3/_2$; (ix) $x, y-1, z$; (x) $-x+{}^1/_2, -y+1, z$; (xi) $-x+{}^1/_2, y+{}^1/_2, -z+{}^1/_2$; (xii) $x, -y+{}^3/_2, -z+{}^1/_2$; (xiii) $-x+{}^1/_2, y-{}^1/_2, -z+{}^1/_2$; (xiv) $x, -y-{}^1/_2, -z+{}^1/_2$).

Table 4. Bond Angles and Torsion Angles (deg) for the Water Heptamer and 1D Water Chains for 1 and 2

Complex **1**	
O3W···O2W^x···O1W	127.0(3)
O2W^x···O1W···O1W^{viii}	136.2(4)
O1W···O1W^{viii}···O1W^{vii}	111.0(4)
O3W···O2W^x···O1W···O1W^{viii}	92.0(7)
O2W^x···O1W···O1W^{viii}···O1W^{vii}	−37.2(8)
O1W···O1W^{viii}···O1W^{vii}···O1W^v	0.4(6)
O4W^v···O4W···O4W^{vi}	112.3(3)
O4W^{xiv}···O4W^{xiii}···O4W^v···O4W	174.3(3)
O4W^{xiii}···O4W^v···O4W···O4W^{vi}	2.2(4)
Complex **2**	
O1W^{iii}···O1W···O2W	130.28(12)
O1W···O2W···O3W	109.15(11)
O2W···O3W···O3W^v	107.74(11)
O3W^{iii}···O2W^{iii}···O1W^{iii}···O1W	26.8(2)
O2W^{iii}···O1W^{iii}···O1W···O2W	180
O1W···O2W···O3W···O3W^v	108.31(13)

Symmetry codes: (v) $-x+{}^1/_2, -y, z$; (vi) $x, -y+{}^1/_2, -z+{}^1/_2$; (vii) $-x+{}^1/_2, y-{}^1/_2, -z+{}^3/_2$; (viii) $x, -y+{}^1/_2, -z+{}^3/_2$; (x) $-x+{}^1/_2, -y+1, z$; (xiii) $-x+{}^1/_2, y-{}^1/_2, -z+{}^1/_2$; (xiv) $x, -y-{}^1/_2, -z+{}^1/_2$. Symmetry codes: (iii) $-x+1, -y+1, -z$; (v) $-x, -y, -z-1$.

The theoretical predictions of low-energy structures of water heptamers suggest that a cuboid structure with a missing corner is found to be the most stable. This structure has ten hydrogen bonds and has a stabilization energy of 60.53 kcal/mol at the HF/6-31G(d,p) level, with a dipole moment (μ) of 1.35 D.[38] Most likely, this is because cage structures maximize the formation of hydrogen bonds within the cluster while interactions with the surrounding environment are ignored.[39] In experiments, high-energy cyclic motifs of water heptamers still can survive in the specific chemical environment which may offer an additional stabilization energy for them. (Symmetry codes: (vii) $-x+{}^1/_2, y-{}^1/_2, -z+{}^3/_2$; (viii) $x, -y+{}^1/_2, -z+{}^3/_2$.)

Adjacent hepamers are reversedly fused together by sharing one edge (O1W···O1W), forming a 1D tape along the *b* axis (Figure 2c). This tape has a width of ca. 11.4 Å and is anchored by ox ligands that undergo hydrogen bonding to O2W and O3W (O2W···O1 = 2.771(10) and O3W···O2 = 2.806(7) Å), giving a $R_3^3(9)$ hydrogen-bonding pattern. According to the water cluster notation, this 1D water tape can be described as a T7(2) classification.

Another water molecule, O4W, does not participate in the heptamer but forms an independent C4 water chain (Figure 2b), which means four water molecules (one O4W and its three crystallographically equivalent neighbors) form the unit cell repeat unit of the chain. Within the water chain, the O4W···O4W separation is 2.796(12) Å, which is slightly longer than the average O···O distances in a heptamer, proving that the linear water chain is less stable than a cyclic one, owing to the formation of less hydrogen bonds within the chain.[14b] The O4W molecules are nearly coplanar, with the torsion angles of O4W^{xiv}···O4W^{xiii}···O4W^v···O4W and O4W^{xiii}···O4W^v···O4W···O4W^{vi} being 174.3(3) and 2.2(4)°, respectively. The O4W acts as a single hydrogen bond donor as well as acceptor in the chain, which also interacts with the ox ligand through the O4W···O2 hydrogen bond (2.789(9) Å). Overall, the 1D water tapes and 1D water chains incorporate the ox ligands to form the anionic 2D sheet (Figure 2c) along the *bc* plane. In other words, as shown in Figure S4, the host−guest relationship between water aggregates and the 3D framework is that the 1D water tapes and the 1D water chains are embedded in the bigger channel A and smaller channel B, respectively, which demonstrates the water aggregates form not only by a simple void-filling but also by the templating effect;[33f,5f] that is to say, the shape and size of the channel in this structure somewhat control the morphologies of the water aggregates. (Symmetry codes: (v) $-x+{}^1/_2, -y, z$; (vi) $x, -y+{}^1/_2, -z+{}^1/_2$; (xiii) $-x+{}^1/_2, y-{}^1/_2, -z+{}^1/_2$; (xiv) $x, -y-{}^1/_2, -z+{}^1/_2$.)

$[Ag_2(bipy)_2(adip)\cdot 6H_2O]_n$ (2). Single crystal X-ray analysis reveals that **2** is an extended 2D sheet involving Ag−bipy double chains and the 1D water chains as guests. As shown in Figure 3a, the asymmetric unit of **2** consists of one crystallographically independent Ag(I) ion, one bipy, half of an adip ligand, and three lattice water molecules. The Ag1 adopts a linear geometry completed by two symmetry independent N atoms from two bipy ligands (Ag1−N1 = 2.2318(19), Ag1−N2^i = 2.2298(17) Å, N2^i−Ag1−N1 = 161.05(8)°), while adip ligand just weakly coordinated to Ag(I) ion with an average Ag···O bond length of 2.7529(19) Å. A pair of adjacent Ag−bipy single chains are linked into a double chain by a weak Ag···Ag contact. The Ag···Ag separation of 3.2146(5) Å in **2** is comparable to those (3.116(1) and 3.286(2) Å) found in two reported infinite molecular ladders ([Ag(bipy)X], X = $MeCO_2^-$ and $H_2PO_4^-$)[40] and those (2.970(2)−3.312(1) Å) found in other Ag(I) CPs with pyridyl−donor ligands,[41] indicating the argentophilic interactions[42] (Symmetry code: (i) $x, y+1, z+1$).

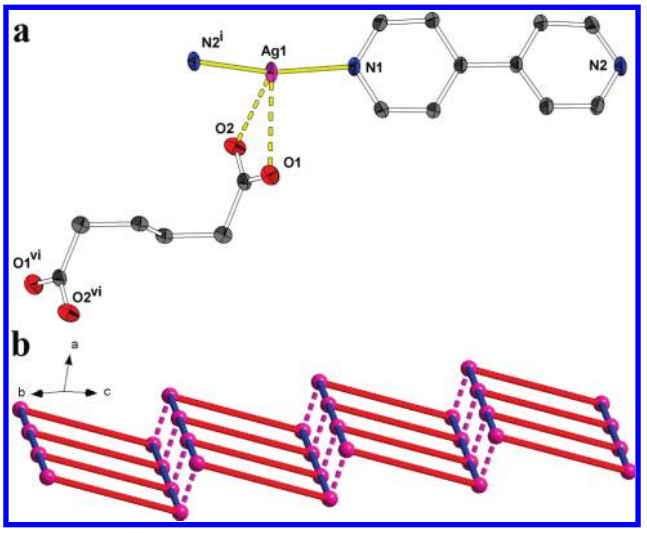

Figure 3. (a) ORTEP plot showing the coordination environment of Ag(I) ion in **2** with the thermal ellipsoids at the 30% probability level. Hydrogen atoms and water molecules are omitted for clarity. (Symmetry codes: (i) $x, y+1, z+1$; (vi) $-x+1, -y+2, -z+1$.) (b) A view of the 2D sheet (red pillar, adip; blue stick, bipy).

The backbone of adip in **2** possesses an *anti−gauche* conformation[43] with the torsion angles of 65.9(10) and 180°. The double chains are linked by adip ligands to form a stairlike 2D sheet through weak Ag···O coordinative bonds (Figure 3b). The pyridyl rings within the double chain are closely stacked with a dihedral angle of 20.25(14)°, and the $\pi\cdots\pi$ contact distance is 3.8654(17) Å (Figure S5 and Table S1), which consolidates the resulting 2D sheet, while the absolutely parallel pyridyl rings between adjacent sheets are stacked together to give a $\pi\cdots\pi$ contact distance of 3.6869(17) Å with the slippage of 1.236 Å, which combines with the rich O_{water}—H···O_{adip} and O_{water}—H···O_{water} hydrogen bonds to play a vital role in the formation of the resulting 3D supramolecular framework.

The most fascinating feature of **2** is that three crystallographically independent lattice water molecules (O1W, O2W, and O3W) within the void are hydrogen bonded to each other, forming an infinite water chain with a curl conformation (Figure 4a). Within the water chain, all water molecules act as a single hydrogen bond donor as well as acceptor. The arrangement mode of three water molecules within a water chain can be described as ···O1W··· O2W···O3W···O3W···O2W···O1W···O1W···O2W ···O3W···. The O···O distances in the chain are in the range 2.831(3)−2.848(5) Å with an average value of 2.840(4) Å, which is longer than that in both the water chain and the water tape of **1**. Moreover, the average O···O···O angle is 115.72(11)°, which is slightly larger than the corresponding value of 109.3° in ice I_h. The overall $[(H_2O)_3]_n$ chain can be represented by C6, according to the water cluster notation. In addition, the O_{water}—H···O_{adip} hydrogen bonds (avg 2.873(3) Å) anchor the water chains to the host adip anions, forming a 2D anionic sheet (Figure 4b). The water aggregates in **1** can be seen as intercalation of guests into voids of the 3D framework host; however, differently, the curl water chains in **2** do not simply fill the voids between the sheets but traverse the $[Ag_4(bipy)_2(adip)_2]$ rectangle grids of the 2D sheets (Figure S6).

Influence of Dicarboxylates on Structures of Both Metal−Organic Frameworks and Water Aggregates. It has been

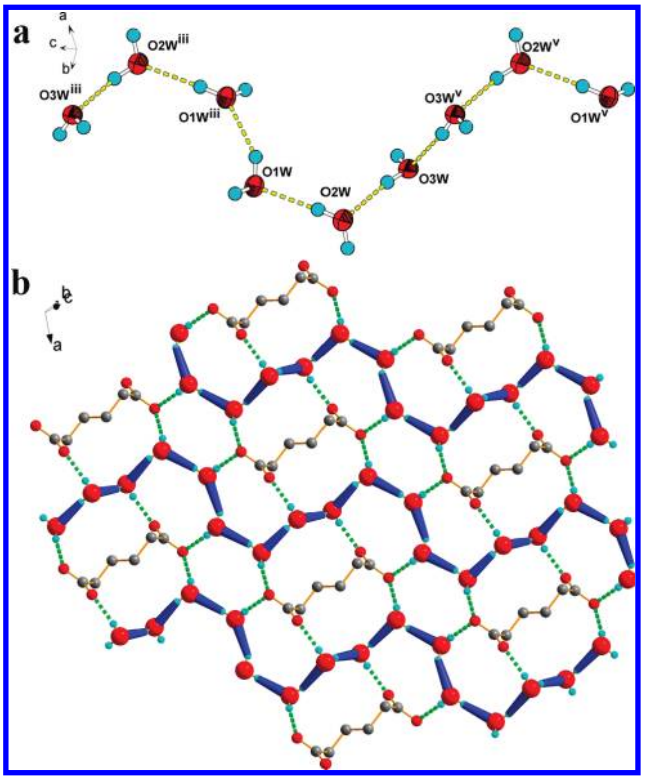

Figure 4. (a) ORTEP plot showing the 1D water chain. (Symmetry codes: (iii) $-x+1, -y+1, -z$; (v) $-x, -y, -z-1$). (b) Ball and stick plot showing the 2D water-adip anionic sheet incorporating the 1D water chain (blue lines). The oxygen atoms of water are shown as bigger balls.

demonstrated that the structural diversities of both metal−organic frameworks and water aggregates in complexes **1** and **2** are undoubtedly related to the configurations and coordination modes of auxiliary dicarboxylates. For **1** and **2**, H_2ox and H_2adip possess rigid and flexible carbon backbones, respectively, as well as the different orientations of carboxylic groups situated in the carbon backbones. For ox anion, it adopts a monodentate bridging mode to sustain the Ag−bipy sheets. Two terminal carboxylic groups do not lie in the same plane and form a large dihedral angle, which makes the Ag−bipy chains in different sheets arrange in a crosslike mode. As a result, the ox pillared 3D framework forms. When replacing short and rigid ox by a long and flexible adip, a 2D sheet was obtained. The bidentate chelating adip anion weakly links Ag(I) ions with an *anti−gauche* conformation to form the resulting 2D sheet. Additionally, as an intermediate member of this series, the previously reported $\{[Ag_3(bipy)_3(suc)_{1.5}]\cdot 10H_2O\}_n$ (H_2suc = succinic acid)[4e] shows a 2D sheet and pillar type of structure based on a Ag···Ag interaction engaged triple Ag−bipy chain where suc ligands adopt two different conformations (*gauche* and *anti−gauche*) and a 1D water tape consisting of $(H_2O)_{18}$ water clusters is observed. These results show diverse dicarboxylates can fine-tune themselves to satisfy the coordination preference of metal centers and the lower energetic arrangement in the self-assembly process. On the other hand, different dicarboxylates not only change the structures of the metal−organic framework but also modulate different hydrophilic environments which are suitable to the various water aggregates being optimally occupied both in terms of packing efficiency and the maximization of intermolecular interactions. Consequently, the morphologies of water

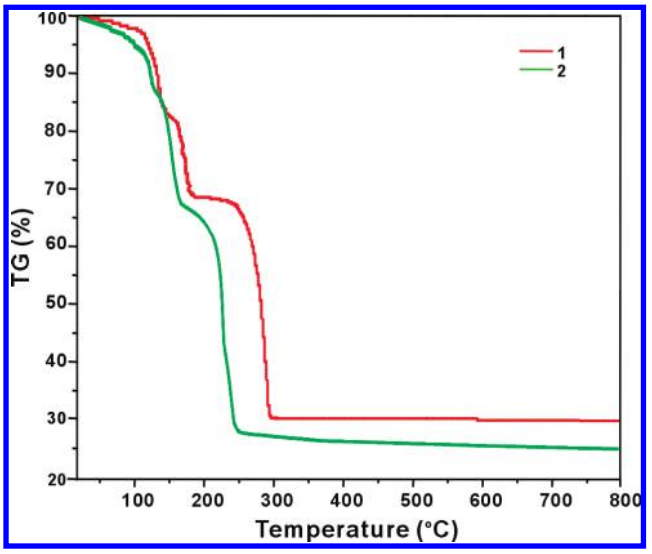

Figure 5. TGA curves for complexes **1** and **2**.

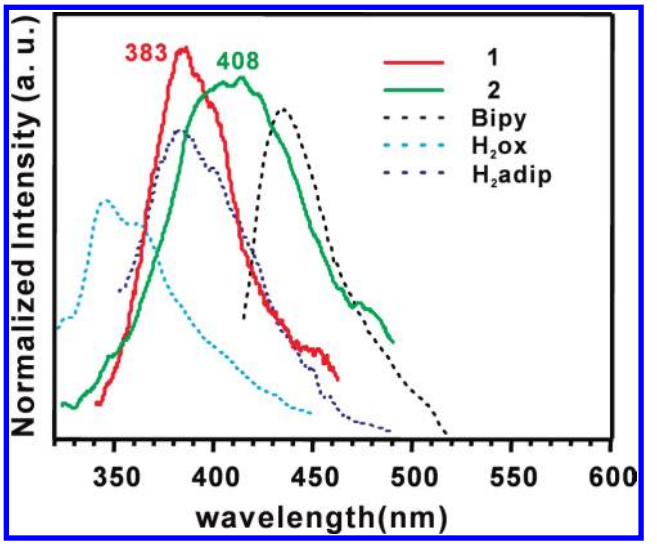

Figure 6. Photoluminescences of free ligands and complexes **1** and **2**.

aggregates are successfully tuned by a change in the shape or distribution of the hydrophilic groups on the host metal−organic frameworks.

TG Analysis. The thermogravimetric (TG) analysis was performed in N_2 atmosphere on polycrystalline samples of complexes **1** and **2**, and the TG curves are shown in Figure 5. The TG curve of **1** shows the first weight loss of 17.95% in the temperature range 25−157 °C, which indicates the loss of seven lattice water molecules per formula unit (calcd: 17.01%), and then the metal−organic framework starts to decompose accompanying loss of organic ligands. The residual weight of 28.81% is consistent with that of 29.07% calculated for metallic silver. For **2**, the weight loss attributed to the gradual release of three water molecules per formula unit is observed in the range 25−130 °C (obsd, 12.99%; calcd, 13.84%) and then the framework collapses in the temperature range 131−249 °C before the final formation of metal silver (obsd, 26.55%; calcd, 27.65%).

Photoluminescence Properties. The photoluminescence spectra of the free ligands and complexes **1** and **2** are shown in Figure 6. The free ligands bipy, H_2ox, and H_2adip display photoluminescence with emission maxima at 436, 342, and 383 nm (λ_{ex} = 300 nm), respectively. It can be presumed that these peaks originate from the $\pi^* \rightarrow$ n or $\pi^* \rightarrow \pi$ transitions. To the best of our knowledge, the emission of dicarboxylate belongs to the $\pi^* \rightarrow$ n transition, which is very weak compared to that of the $\pi^* \rightarrow \pi$ transition of the bipy, so the dicarboxylates almost have no contribution to the fluorescent emission of as-synthesized CPs.[44] Upon complexation of these ligands with Ag(I) ions, intense emissions are observed at 383 nm (λ_{ex} = 300 nm) for **1** and 408 nm (λ_{ex} = 310 nm) for **2**, respectively. The resemblance between the emissions of **1** and **2** and that of the free bipy indicates that the emissions of **1** and **2** originate from the $\pi^* \rightarrow \pi$ electronic transition of bipy ligand.[45] In comparison with **1**, a red shift of 25 nm has been observed in **2** which can be attributed to the combination of replacement of ox by adip and the existence of the Ag···Ag interaction in **2**.[46]

Conclusions

In summary, we have succeeded in modulating not only the structural motifs of the metal−organic framework but also the 1D water aggregates including a 1D water tape, a 1D C4 water chain, as well as a 1D C6 water chain by employment of different aliphatic dicarboxylates. The heptamer water cluster, the subunit of the 1D water tape in **1**, provides a rare example of a high-nuclearity, odd-numbered water cluster very different from the one found experimentally or predicted theoretically. Including the 1D water tape, a 1D water chain also exists in **1**, which is different from that in **2**. These results illustrate the structural diversity of water aggregates and the sensitive dependence of their structures upon the details of their environment. The precise structural analysis and the cooperative association of the water aggregates and crystal hosts may provide insight into the hydrogen-bonding motif of the aqueous environment in living systems and a clear understanding of the structure of ice and bulk water as well.

Acknowledgment. This work was financially supported by the National Natural Science Foundation of China (No. 20721001), 973 Project (Grant 2007CB815301) from MSTC, and The National Science Fund of China for Fostering Talents in Basic Science (No. J0630429).

Supporting Information Available: Crystallographic data in CIF format and additional figures of the structures, powder X-ray diffraction (PXRD) patterns, and IR spectra for **1** and **2**. This material is available free of charge via the Internet at http://pubs.acs.org.

References

(1) (a) Ludwig, R. *Angew. Chem., Int. Ed.* **2001**, *40*, 1808–1827. (b) Ball, P. *H_2O: A Biography of Water*; Weidenfeld & Nicolson: London, 1999. (c) Debenedetti, P. G. *Metastable Liquids*; Princeton University Press: Princeton, 1996. (d) Dorsey, E. *Properties of Ordinary Water Substance*; American Chemical Society Monograph Series; New York, 1968. (e) Liu, K.; Cruzan, J. D.; Saykally, R. J. *Science* **1996**, *271*, 929–933. (f) Liu, K.; Brown, M. G.; Cruzan, J. D.; Saykally, R. J. *Science* **1996**, *271*, 62–64. (g) Cruzan, J. D.; Braly, L. B.; Liu, K.; Brown, M. G.; Loeser, J. G.; Saykally, R. J. *Science* **1996**, *271*, 59–62. (h) Liu, K.; Brown, M. G.; Carter, C.; Saykally, R. J.; Gregory, J. K.; Clary, D. C. *Nature* **1996**, *381*, 501–503. (i) Pugliano, N.; Saykally, R. J. *Science* **1992**, *257*, 1937–1940. (j) Smith, J. D.; Cappa, C. D.; Wilson, K. R.; Messer, B. M.; Cohen, R. C.; Saykally, R. J. *Science* **2004**, *306*, 851–853. (k) Keutsch, F. N.; Cruzan, J. D.; Saykally, R. *J. Chem. Rev.* **2003**, *103*, 2533–2577. (l) Nauta, K.; Miller, R. E. *Science* **2000**, *287*, 293–295.

(2) (a) Bi, Y.; Liao, W.; Zhang, H.; Li, D. *CrystEngComm* **2009**, *11*, 1213–1216. (b) Pan, Q. H.; Li, J. Y.; Christensen, K. E.; Bonneau, C.;

Ren, X. Y.; Shi, L.; Sun, J. L.; Zou, X. D.; Li, G. H.; Yu, J. H.; Xu, R. R. *Angew. Chem., Int. Ed.* **2008**, *47*, 7868–7871. (c) Mimura, M.; Matsuo, T.; Nakashima, T.; Matsumoto, N. *Inorg. Chem.* **1998**, *37*, 3553–3560. (d) Das, M. C.; Bharadwaj, P. K. *Eur. J. Inorg. Chem.* **2007**, 1229–1232. (e) Xie, Y. S.; Ni, J.; Zheng, F. K.; Cui, Y.; Wang, Q. G.; Ng, S. W.; Zhu, W. H. *Cryst. Growth Des.* **2009**, *9*, 118–126. (f) Custalcean, R.; Afloroaiei, C.; Vlassa, M.; Polverejan, M. *Angew. Chem., Int. Ed.* **2000**, *39*, 3094–3096. (g) Lakshminarayanan, P. S.; Suresh, E.; Ghosh, P. *Angew. Chem., Int. Ed.* **2006**, *45*, 3807–3811. (h) Cheng, L.; Lin, J. B.; Gong, J. Z.; Sun, A. P.; Ye, B. H.; Chen, X. M. *Cryst. Growth Des.* **2006**, *6*, 2739–2746. (i) Fabelo, O.; Pasán, J.; Cañadillas-Delgado, L.; Delgado, F. S.; Labrador, A.; Lloret, F.; Julve, M.; Ruiz-Pérez, C. *CrystEngComm* **2008**, *10*, 1743–1746. (j) Xu, W. Z.; Sun, J. L.; Huang, Z. T.; Zheng, Q. Y. *Chem. Commun.* **2009**, 171–173. (k) Henry, M.; Taulelle, F.; Loiseau, T.; Beitone, L.; Férey, G. *Chem.—Eur. J.* **2004**, *10*, 1366–1372. (l) Wan, Y. H.; Zheng, X. J.; Wang, F. Q.; Zhou, X. Y.; Wang, K. Z.; Jin, L. P. *CrystEngComm* **2009**, *11*, 278–283. (m) Dai, F. N.; He, H. Y.; Sun, D. F. *J. Am. Chem. Soc.* **2008**, *130*, 14064–14065. (n) Raghuraman, K.; Katti, K. K.; Barbour, L. J.; Pillarsetty, N.; Barnes, C. L.; Katti, K. V. *J. Am. Chem. Soc.* **2003**, *125*, 6955–6961. (o) Sang, R. L.; Xu, L. *CrystEngComm* **2010**, *12*, 1377–1381. (p) Luan, X.; Chu, Y.; Wang, Y.; Li, D.; Liu, P.; Shi, Q. Z. *Cryst. Growth Des.* **2006**, *6*, 812–814.

(3) (a) Mukherjee, A.; Saha, M. K.; Nethaji, M.; Chakravarty, A. R. *Chem. Commun.* **2004**, 716–717. (b) Fei, Z.; Zhao, D.; Geldbach, T. J.; Scopelliti, R.; Dyson, P. J.; Antonijevic, S.; Bodenhausen, G. *Angew. Chem., Int. Ed.* **2005**, *44*, 5720–5725. (c) Saha, B. K.; Nangia, A. *Chem. Commun.* **2005**, 3024–3026. (d) Cui, Y.; Cao, M. L.; Yang, L. F.; Niu, Y. L.; Ye, B. H. *CrystEngComm* **2008**, *10*, 1288–1290. (e) Natarajan, R.; Charmant, J. P. H. A.; Orpen, G.; Davis, A. P. *Angew. Chem., Int. Ed.* **2010**, *49*, 5125–5129.

(4) (a) Ma, B. Q.; Sun, H. L.; Gao, S. *Chem. Commun.* **2005**, 2336–2338. (b) Tadokoro, M.; Fukui, S.; Kitajima, T.; Nagao, Y.; Ishimaru, S.; Kitagawa, H.; Isobee, K.; Nakasuji, K. *Chem. Commun.* **2006**, 1274–1276. (c) Custelcean, R.; Afloroaei, C.; Vlassa, M.; Polverejan, M. *Angew. Chem., Int. Ed.* **2000**, *39*, 3094–3096. (d) Shi, X. F.; Song, H. B.; He, L.; Zhang, W. Q. *CrystEngComm* **2009**, *11*, 542–544. (e) Li, F.; Li, T.; Yuan, D.; Lv, J.; Cao, R. *Inorg. Chem. Commun.* **2006**, *9*, 691–694.

(5) (a) Janiak, C.; Scharamann, T. G.; Mason, S. A. *J. Am. Chem. Soc.* **2002**, *124*, 14010–14011. (b) Oxtoby, N. S.; Blake, A. J.; Champness, N. R.; Wilson, C. *Chem.—Eur. J.* **2005**, *11*, 4643–4654. (c) Fei, Z. F.; Geldbach, T. J.; Zhao, D. B.; Scopelliti, R.; Dyson, P. J. *Inorg. Chem.* **2005**, *44*, 5200–5202. (d) Rodríguez-Cuamatzi, P.; Vargas-Díaz, G.; Höpfl, H. *Angew. Chem., Int. Ed.* **2004**, *43*, 3041–3044. (e) Zhang, J. P.; Huang, X. C.; Lin, Y. Y.; Chen, X. M. *Inorg. Chem.* **2005**, *44*, 3146–3150. (f) Luan, X. J.; Chu, Y. C.; Wang, Y. Y.; Li, D. S.; Liu, P.; Shi, Q. Z. *Cryst. Growth Des.* **2006**, *6*, 812–814. (g) Lakshminarayanan, P. S.; Suresh, E. I.; Ghost, P. *J. Am. Chem. Soc.* **2005**, *127*, 13132–13133. (h) Yang, A. H.; Zhang, H.; Gao, H. L.; Zhang, W. Q.; He, L.; Cui, J. Z. *Cryst. Growth Des.* **2008**, *8*, 3354–3359.

(6) (a) Carballo, R.; Covelo, B.; Lodeiro, C.; Vázquez-López, E. M. *CrystEngComm* **2005**, *7*, 294–296. (b) Carballo, R.; Covelo, B.; Fernández-Hermida, N.; García-Martínez, E.; Lago, A. B.; Vázquez, M.; Vázquez-López, E. M. *Cryst. Growth Des.* **2006**, *6*, 629–631. (c) Li, C. H.; Huang, K. L.; Dou, J. M.; Chi, Y. N.; Xu, Y. Q.; Shen, L.; Wang, D. Q.; Hu, C. W. *Cryst. Growth Des.* **2008**, *8*, 3141–4143.

(7) (a) Long, L. S.; Wu, Y. R.; Huang, R. B.; Zheng, L. S. *Inorg. Chem.* **2004**, *43*, 3798–3800. (b) Zuhayra, M.; Kampen, W. U.; Henze, E.; Soti, Z.; Zsolnai, L.; Huttner, G.; Oberdorfer, F. A. *J. Am. Chem. Soc.* **2006**, *128*, 424–425.

(8) (a) Wang, J.; Zheng, L.-L.; Li, C.-J.; Zheng, Y.-Z.; Tong, M.-L. *Cryst. Growth Des.* **2006**, *6*, 357–359. (b) Ghosh, S. K.; Bharadwaj, P. K. *Inorg. Chem.* **2003**, *42*, 8250–8254. (c) Luna-García, R.; Damián-Murillo, B. M.; Barba, V.; Höpfl, H.; Beltrán, H. I.; Zamudio-Rivera, L. S. *Chem. Commun.* **2005**, 5527–5529.

(9) (a) Atwood, J. L.; Barbour, L. J.; Ness, T. J.; Raston, C. J.; Raston, P. L. *J. Am. Chem. Soc.* **2001**, *123*, 7192–7193. (b) Khatua, S.; Kang, J.; Huh, J. O.; Hong, C. S.; Churchill, D. G. *Cryst. Growth Des.* **2010**, *10*, 327–334. (c) Maxim, C.; Sorace, L.; Khuntia, P.; Madalan, A. M.; Kravtsov, V.; Lascialfari, A.; Caneschi, A.; Journaux, Y.; Andruh, M. *Dalton Trans.* **2010**, *39*, 4838–4847.

(10) (a) Barbour, L. J.; Orr, G. W.; Atwood, J. L. *Nature* **1998**, *393*, 671–673. (b) Barbour, L. J.; Orr, G. W.; Atwood, J. L. *Chem. Commun.* **2000**, 859–860. (c) Yoshizawa, M.; Kusukawa, T.; Kawano, M.; Ohhara, T.; Tanaka, I.; Kurihara, K.; Niimura, N.; Fujita, M. *J. Am. Chem. Soc.* **2005**, *127*, 2798–2799.

(11) (a) Ma, B.-Q.; Sun, H.-L.; Gao, S. *Angew. Chem., Int. Ed.* **2004**, *43*, 1374–1376. (b) Ghosh, S. J.; Bharadwaj, P. K. *Angew. Chem., Int. Ed.* **2004**, *43*, 3577–3580. (c) Wang, X.; Lin, H.; Mu, B.; Tian, A.; Liu, G. *Dalton Trans.* **2010**, *39*, 6187–6189. (d) Neogi, S.; Savitha, G.; Bharadwaj, P. K. *Inorg. Chem.* **2004**, *43*, 3771–3773. (e) Song, H. H.; Ma, B. Q. *CrystEngComm* **2007**, *9*, 625–627.

(12) Ghosh, S. K.; Ribas, J.; Fallah, M. S. E.; Bharadwaj, P. K. *Inorg. Chem.* **2005**, *44*, 3856–3862.

(13) Ghosh, S. K.; Bharadwaj, P. K. *Inorg. Chem.* **2004**, *43*, 6887–6889.

(14) (a) MacGillivray, L. R.; Atwood, J. L. *J. Am. Chem. Soc.* **1997**, *119*, 2592–2593. (b) Ghosh, S. K.; Bharadwaj, P. K. *Inorg. Chem.* **2005**, *44*, 5553–5555.

(15) (a) Ma, B. Q.; Sun, H. L.; Gao, S. *Chem. Commun.* **2004**, 2220–2222. (b) Day, M. B.; Kirschner, K. N.; Shields, G. C. *J. Phys. Chem. A* **2005**, *109*, 6773–6778.

(16) Mir, M. H.; Vittal, J. J. *Angew. Chem., Int. Ed.* **2007**, *46*, 5925–5928.

(17) (a) Buck, U.; Huisken, F. *Chem. Rev.* **2000**, *100*, 3863–3890. (b) Brudermann, J.; Melzzer, M.; Buck, U.; Kazmirski, J. K.; Sadlej, J.; Buch, V. *J. Chem. Phys.* **1999**, *110*, 10649–10652.

(18) (a) Kim, J.; Majumbur, D.; Lee, H. M.; Kim, K. S. *J. Chem. Phys.* **1999**, *110*, 9128–9134. (b) Kryachko, E. S. *Chem. Phys. Lett.* **1997**, *272*, 132–138. (c) Jensen, J. O.; Krishnan, P. N.; Burke, L. A. *Chem. Phys. Lett.* **1995**, *241*, 253–260.

(19) (a) Westhoff, E. *Water and Biological Macromolecules*; CRC: Boca Raton, FL, 1993. (b) Sainz, G.; Carrell, C. J.; Ponamerev, M. V.; Soriano, G. M.; Cramer, W. A.; Smith, J. L. *Biochemistry* **2000**, *39*, 9164–9173. (c) Tajkhorshid, K.; Nollert, P.; Jensen, M. Ø.; Miercke, L. J. W.; O'Connell, J.; Stroud, R. M.; Schulten, K. *Science* **2002**, *296*, 525–530.

(20) (a) Li, M.; Chen, S.-P.; Xiang, J.-F.; He, H.-J.; Yuan, L.-J.; Sun, J.-T. *Cryst. Growth Des.* **2006**, *6*, 1250–1252. (b) Reger, D. L.; Semeniuc, R. F.; Pettinari, C.; Luna-Giles, F.; Smith, M. D. *Cryst. Growth Des.* **2006**, *6*, 1068–1070. (c) Shi, X.-F.; Zhang, W.-Q. *Cryst. Growth Des.* **2007**, *7*, 595–597.

(21) (a) Infantes, L.; Motherwell, S. *CrystEngComm* **2002**, *4*, 454–461. (b) Infantes, L.; Chisholm, J.; Motherwell, S. *CrystEngComm* **2003**, *5*, 480–486. (c) Mascal, M.; Infantes, L.; Chisholm, J. *Angew. Chem., Int. Ed.* **2006**, *45*, 32–36.

(22) Wang, Y. T.; Tang, G. M.; Liu, Z. M.; Yi, X. H. *Cryst. Growth Des.* **2007**, *7*, 2272–2275.

(23) (a) Sun, D.; Zhang, N.; Xu, Q. J.; Luo, G. G.; Huang, R. B.; Zheng, L. S. *J. Mol. Struct.* **2010**, *969*, 176–181. (b) Sun, D.; Luo, G. G.; Zhang, N.; Huang, R. B.; Zheng, L. S. *Acta Crystallogr. C* **2009**, *65*, m418–m421. (c) Sun, D.; Yang, C. F; Wei, Z. H.; Luo, G. G.; Zhang, N.; Xu, Q. J.; Huang, R. B.; Zheng, L. S. *Z. Naturforsch.* **2010**, *65b*, 152–156.

(24) Higashi, T. *ABSCOR, Empirical Absorption Correction based on Fourier Series Approximation*; Rigaku Corporation: Tokyo, 1995.

(25) Sheldrick, G. M. *SHELXS-97, Program for X-ray Crystal Structure Determination*; University of Gottingen: Germany, 1997.

(26) Sheldrick, G. M. *SHELXL-97, Program for X-ray Crystal Structure Refinement*; University of Gottingen: Germany, 1997.

(27) Spek,A. L. *Implemented as the PLATON Procedure, a Multipurpose Crystallographic Tool*; Utrecht University: Utrecht, The Netherlands, 1998.

(28) (a) Sun, D. F.; Cao, R.; Bi, W. H.; Hong, M. C.; Chang, Y. L. *Inorg. Chim. Acta* **2004**, *357*, 991–1001. (b) Smith, G.; Reddy, A. N.; Byriel, K. A.; Kennard, C. H. L. *J. Chem. Soc., Dalton Trans.* **1995**, 3565–3570.

(29) (a) Sun, D.; Luo, G. G.; Zhang, N.; Wei, Z. H.; Yang, C. F.; Xu, Q. J.; Huang, R. B.; Zheng, L. S. *Chem. Lett.* **2010**, *39*, 190–191. (b) Hao, H. Q.; Liu, W. T.; Tan, W.; Lin, Z. J.; Tong, M. L. *Cryst. Growth Des.* **2009**, *9*, 457–465.

(30) (a) Nakamoto, K. *Infrared and Raman Spectra of Inorganic and Coordination Compounds*; John Wiley & Sons: New York, 1986. (b) Deacon, G. B.; Phillips, R. J. *Coord. Chem. Rev.* **1980**, *33*, 227–250.

(31) (a) Bondi, A. *J. Phys. Chem.* **1964**, *68*, 411–451. (b) Lian, Z. X.; Cai, J. W.; Chen, C. H.; Luo, H. B. *CrystEngComm.* **2007**, *9*, 319–327.

(32) (a) Degtyarenko, A. S.; Solntsev, P. V.; Krautscheid, H.; Rusanov, E. B.; Chernega, A. N.; Domasevitch, K. V. *New J. Chem.* **2008**, *32*, 1910–1918. (b) Gural'skiy, I. A.; Solntsev, P. V.; Krautscheid, H.; Domasevitch, K. V. *Chem. Commun.* **2006**, 4808–4810. (c) Kong, X. J.; Ren, Y. P.; Zheng, P. Q.; Long, Y. X.; Long, L. S.; Huang, R. B.; Zheng, L. S. *Inorg. Chem.* **2006**, *45*, 10702–10711. (d) Gural'skiy, I. A.; Escudero, D.; Frontera, A.; Solntsev, P. V.; Rusanov, E. B.; Chernega, A. N.; Krautscheid, H.; Domasevitch, K. V. *Dalton Trans.* **2009**, 2856–2864. (e) Domasevitch, K. V.; Solntsev, P. V.; Gural'skiy, I. A.; Krautscheid,

H.; Rusanov, E. B.; Chernega, A. N.; Howard, J. A. K. *Dalton Trans.* **2007**, 3893–3905. (f) Boldog, I.; Daran, J.-C.; Chernega, A. N.; Rusanov, E. B.; Krautscheid, H.; Domasevitch, K. V. *Cryst. Growth. Des.* **2009**, *9*, 2895–2905. (g) Boldog, I.; Rusanov, E. B.; Sieler, J.; Blaurock, S.; Domasevitch, K. V. *Chem. Commun.* **2003**, 740–741. (h) Carballo, R.; Covelo, B.; Fernández-Hermida, N.; Lago, A. B.; Vázquez-López, E. M. *Polyhedron* **2009**, *28*, 923–932.

(33) Allen, F. H. *Acta Crystallogr., Sect. B: Struct. Sci.* **2002**, *58*, 380–388.

(34) Tong, M L.; Wu, Y. M.; Ru, J.; Chen, X. M.; Chang, H. C.; Kitagawa, S. *Inorg. Chem.* **2002**, *41*, 4846–4848.

(35) (a) Sun, D.; Luo, G. G.; Xu, Q. J.; Zhang, N.; Jin, Y. C.; Zhao, H. X.; Lin, L. R.; Huang, R. B.; Zheng, L. S. *Polyhedron* **2009**, *28*, 2983–2988. (b) Sun, D.; Luo, G. G.; Zhang, N.; Xu, Q. J.; Huang, R. B.; Zheng, L. S. *Polyhedron* **2010**, *29*, 1243–1250.

(36) Bernstein, J.; Davis, R. E.; Shimoni, L.; Chang, N.-L. *Angew. Chem., Int. Ed. Engl.* **1995**, *34*, 1555–1573.

(37) Zaworotko, M. J. *Chem. Soc. Rev.* **1994**, *23*, 283–288.

(38) Maheshwary, S.; Patel, N.; Sathyamurthy, N.; Kulkarni, A. D.; Gadre, S. R. *J. Phys. Chem. A* **2001**, *105*, 10525–10537.

(39) Atwood, J. L.; Barbour, L. J.; Ness, T. J.; Raston, C. L.; Raston, P. L. *J. Am. Chem. Soc.* **2001**, *123*, 7192–7193.

(40) Tong, M.-L.; Chen, X.-M.; Ng, S. W. *Inorg. Chem. Commun.* **2000**, *3*, 436–441.

(41) (a) Pan, L.; Woodlock, E. B.; Wang, X.; Lam, K.-C.; Rheingold, A. L. *Chem. Commun.* **2001**, 1762. (b) Robinson, F.; Zaworotko, M. *J. Chem. Soc., Chem. Commun.* **1995**, 2413. (c) Yaghi, O. M.; Li, H. *J. Am. Chem. Soc.* **1996**, *118*, 295. (d) Withersby, M. A.; Blake, A. J.; Champness, N. R.; Hubberstey, P.; Li, W.-S.; Schröder, M. *Angew. Chem., Int. Ed. Engl.* **1997**, *36*, 2327. (e) Carlucci, L.; Ciani, G.; Macchi, P.; Proserpio, D. M. *Chem. Commun.* **1998**, 1837. (f) Tong, M.-L.; Chen, X.-M.; Ye, B.-H.; Ng, S. W. *Inorg. Chem.* **1998**, *37*, 5278.

(42) Pyykkö, P. *Chem. Rev.* **1997**, *97*, 597–636.

(43) Rather, B.; Zaworotko, M. J. *Chem. Commun.* **2003**, 830–831.

(44) Chen, W. J.; Wang, Y.; Chen, C.; Yue, Q.; Yuan, H. M.; Chen, J. S.; Wang, S. N. *Inorg. Chem.* **2003**, *42*, 944–946.

(45) Li, F. F.; Ma, J. F.; Song, S. Y.; Yang, J.; Jia, H. Q.; Hu, N. H. *Cryst. Growth Des.* **2006**, *6*, 209–215.

(46) Yi, L.; Zhu, L.-N.; Ding, B.; Cheng, P.; Liao, D.-Z.; Yan, S.-P.; Jiang, Z.-H. *Inorg. Chem. Commun.* **2003**, *6*, 1209–1212.